

## LASER-EXCITED THERMOACOUSTIC ARRAYS

C. R. Culbertson, T. G. Muir, and J. R. Clynh

Applied Research Laboratories  
The University of Texas at Austin  
Austin, Texas 78712 U.S.A.

The generation of sound by the absorption of light has been studied since the 1880's.<sup>1,2</sup> Recently several methods for generating sound with lasers have been examined.<sup>3-8</sup> Westervelt and Larson<sup>1</sup> have proposed one such method that is of potential significance in underwater acoustics. Their results can be used to show that highly directive sound beams of low frequency can be created by the thermalization process in water.

This paper reports the experimental validation of the Westervelt-Larson theory.

Theoretical Summary

The original concept of the laser-excited thermoacoustic array is illustrated in Fig. 1a. A laser radiates an amplitude modulated beam of cross sectional area  $S_0$  that is injected into an absorptive medium at the origin, and propagates in the  $+z$  direction. A hypothetical three cycle pulse propagating at the speed of light in the presence of exponential absorption is shown in Fig. 1b. Each elemental volume in the irradiated medium experiences a stairstep rise in temperature in sympathy with the light modulation. This leads to an oscillatory expansion in the thermal volume.

The acoustic pressure field radiated by this mechanism is predicted by<sup>1,9</sup>

$$P(\vec{r}) = - \frac{i\omega\beta I_0}{8\pi c_p} e^{i\omega t} \int e^{-\alpha z} \frac{e^{ik|\vec{r}-\vec{r}'|}}{|\vec{r}-\vec{r}'|} d^3r', \quad (1)$$

where  $\alpha$  = the optical absorption coefficient,  $\omega$  = angular modulation frequency,  $\beta$  = logarithmic coefficient of thermal expansion,  $c_p$  = specific heat per unit mass,  $I_0$  = output intensity of the laser,<sup>9</sup> and  $\vec{r}$  and  $\vec{r}'$  follow from Fig. 1.

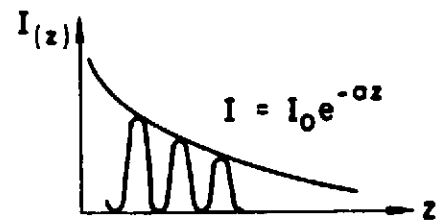
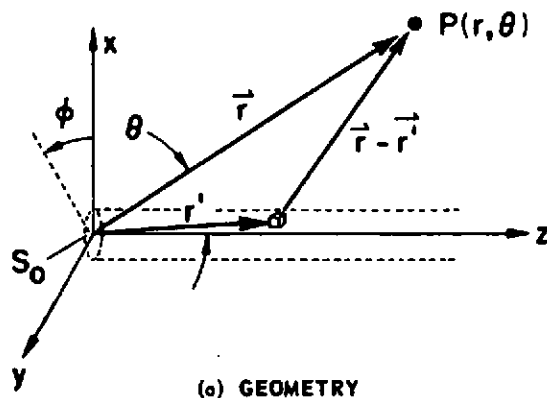


FIGURE 1  
PRINCIPLE OF THE THERMOACOUSTIC ARRAY

The farfield solution to Eq. (1), for the case of a small laser beam ( $\sqrt{S_0/\pi} < \lambda$ ) is

$$p = - \frac{i\omega\beta P_0}{8\pi r c_p} \frac{e^{ikr-i\omega t}}{\alpha + ik \cos \theta} \quad (2)$$

where  $P_0$  is the unmodulated laser power.

From Eq. (2) follows the directivity function,

$$D(\theta) = \frac{\alpha_T}{(\alpha_T^2 + k^2 \cos^2 \theta)^{1/2}} \quad (3)$$

where  $\alpha_T$  = the total attenuation coefficient, and the source level referred to 1 m is

$$L_s = 20 \log \frac{f\beta P_0}{4c_p} \quad (4)$$

The predicted farfield half-power angle of the thermoacoustic array is

$$\theta_{1/2} = \frac{180}{\pi} \left( \frac{\alpha_T}{k} \right) \quad (5)$$

where  $\theta_{1/2}$  is the angle (in degrees) at which the power is reduced by one half from its value on the acoustic axis.

The great speed of light in comparison to that of sound leads to practically instantaneous dynamic excitation of each elemental volume. This makes the array a broadside radiator, having a beamwidth inversely proportional to the length of the absorption limited path of the light beam. This array is also shaded with an exponential taper by the optical attenuation of the medium, so that the acoustic radiation is devoid of minor lobes. For the configuration shown in Fig. 1a, the radiation is omnidirectional in the xy plane, and is centered at the origin.

## Experimental Apparatus

A schematic of the modulated laser system used in these experiments is shown in Fig. 2

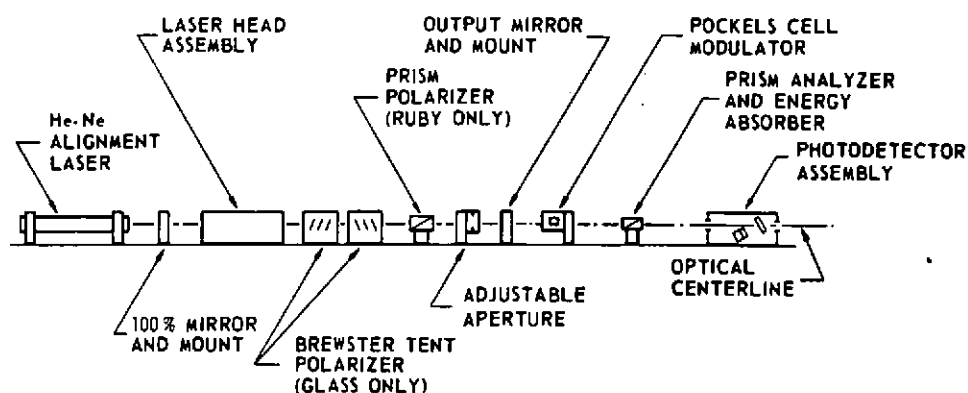


FIGURE 2  
MODULATED LASER SYSTEM

The laser head assembly contains a helical flashlamp and either a Neodymium glass rod (infrared light at  $1.06 \mu\text{m}$ ) or a ruby rod (red light at  $0.6943 \mu\text{m}$ ). A Brewster stack is used to polarize the output of the Nd:glass rod, and a calcite prism polarizer is used with the ruby rod. A 100% back mirror and output mirror complete the optical cavity.

The intensity of the light produced by this cavity is modulated by a Pockels cell and prism analyzer according to

$$I = I_0 \left( \frac{1}{2} - \frac{1}{2} \cos \omega t \right) \quad (6)$$

The modulated laser pulse is monitored by a photodetector, and travels through an optical standpipe equipped with prisms, irises, and a window necessary for beam deflection, control, and transmission and enters the water in a horizontal plane.

A 17 in. diameter line-in-cone hydrophone,<sup>10</sup> located in the plane of the laser beam, was used to receive the acoustic signals.

The experiments were conducted in the freshwater of Lake Travis, near Austin, Texas, U.S.A.

## Existence Test

The first experiment was to determine if the thermoacoustic array produced an acoustic signal. The laser was modulated at 20 kHz for a pulselength of 1 msec and fired into the water. An acoustic signal was produced at the hydrophone which agreed in frequency, pulse length, and time of arrival for the distance traveled between the optical standpipe and the hydrophone.

When the laser was fired into an absorber inserted on the system's optical axis, no acoustic signal was received at the hydrophone. This existence test confirms that the acoustic signal was generated in the water and not in the experimental apparatus.

### Beam Formation

The second measurement tested the prediction that a sound beam is formed by the thermoacoustic array. Fig. 3 shows a farfield beampattern taken at 50 kHz with the Nd:glass laser. The pattern was acquired at a range of 16.8 m, when the measured<sup>11</sup> optical attenuation  $\alpha_T$  was  $15.7 \text{ m}^{-1}$ . A comparison is shown in Fig. 3 between the measured pattern and a plot of  $D(\theta)$ , predicted by Eq. (3). It can be seen that a beam was indeed formed perpendicular to the optical axis with a beamwidth between half power points of  $9.5^\circ$ . This compares well to a theoretical  $8.5^\circ$  beamwidth, considering the pulse-to-pulse variations in the output of the laser, and the variations due to reflections off the optical standpipe.

### Beamwidth Frequency Response

Measurements of  $\theta_{1/2}$  for different modulation frequencies of the

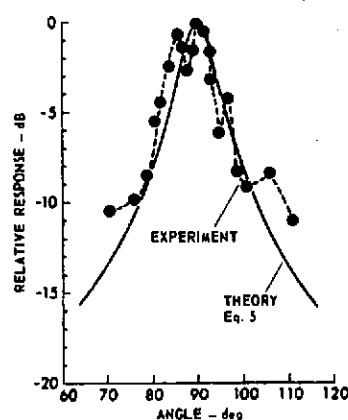


FIGURE 3  
FARFIELD BEAMPATTERN

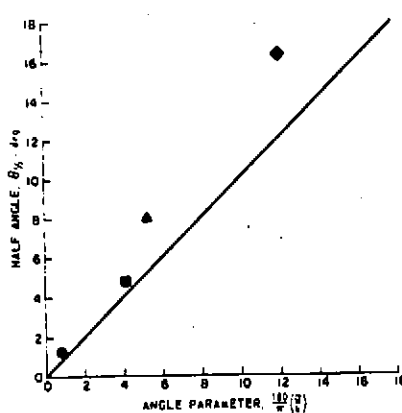


FIGURE 4  
HALF POWER ANGLE

ruby and Nd:glass laser systems are compared in Fig. 4 to the values predicted by Eq. (5). The data demonstrate an increase of beamwidth with increase in optical attenuation and decrease in acoustic frequency, as predicted by theory. The tendency of the measured half-power angles to be broader than theory in the large angle range is primarily due to reflections off the optical standpipe.

### Source Level

Measurements of sound pressure produced by the thermoacoustic array were made as a function of laser power, using the Nd:glass system. The

modulation frequency was 20 kHz and the hydrophone was on the acoustic axis at a range of 10.3 m. The results are presented in Fig. 5 in terms of rms source level. Since the thermoacoustic pressure depends on the optical power delivered to the medium, it was necessary to account for the optical losses in the path of the light beam following the photodetector. Also important are an acoustic diffraction loss due to the finite radius of the thermoacoustic volume and an optical scattering loss in the medium. Taking into account these effects,<sup>11</sup> the theoretical source level is calculated from Eq. (4), and the results are compared in Fig. 5 to measured source level.

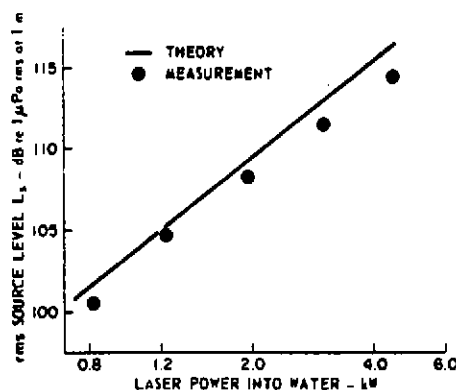


FIGURE 5  
SOURCE LEVEL DEPENDENCE ON OPTICAL POWER

In accordance with Eq. (4), a linear-log plot of  $L_s$  versus optical power should be a straight line with a slope of 6 dB per doubling of power. This expectation is borne out by the data shown in Fig. 5 to within experimental accuracy. Agreement between absolute levels of the theoretical and experimental values is also quite reasonable.

#### Finite Beam Effects

Due to divergence, high-power laser beam diameters encountered in practice are frequently comparable to an acoustic wavelength. For such finite beam diameters, an acoustic diffraction effect within the thermal volume arises when sound waves generated in different regions of this volume do not arrive in phase at remote points in the field. The loss in source level due to the finite size of the laser beam can be presented by<sup>12</sup>

$$\Delta L_s = 20 \log \frac{2}{w^2} \int_0^a J_0(kx) \exp\left(\frac{-x^2}{w^2}\right) x dx \quad , \quad (7)$$

where  $a$  is the radius of the limiting optical aperture,  $J_0(\cdot)$  is the zero Bessel function of argument  $(\cdot)$ , and  $w$  is a "spot size parameter" that specified the  $\frac{1}{e}$  half width of laser beam with gaussian intensity cross section.

A measurement of relative SPL versus aperture radius was conducted on the acoustic axis of a 50 kHz sound beam produced by the Nd:glass system. The results, normalized with respect to the theoretical curve, are compared in Fig. 6 to a plot of Eq. (7). It can be seen that an optimum setting exists for the aperture radius somewhere between the fully opened position, where the effects of diffraction are dominant, and the fully stopped position, where reductions in transmitted laser power dominate. The agreement in the slope of the theoretical and experimental curves is quite reasonable, especially near the optimum setting, and this suggests the utility of Eq. (7) in array design.

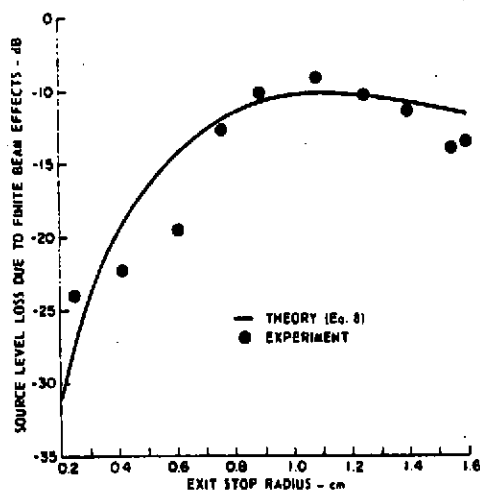


FIGURE 6  
FINITE BEAM EFFECT

### Nearfield Effects

Predictions of nearfield thermoacoustic amplitude and angular response can be made by numerical integration of Eq. (1). Results from a calculation of half-power angle as a function of range for a typical situation (ruby laser modulated at 20 kHz) are shown in Fig. 7. The curve shown asymptotically approaches the farfield angle predicted by Eq. (5), and at a range  $x = 3(k/\alpha^2)$  the calculated angle approaches to within one dB of its farfield value. Thus the  $3K/\alpha^2$  range can therefore be thought of as a convenient demarcation between near and farfield regions.

The nearfield beampattern shown in Fig. 8 was taken at a range of 29.3 m with the ruby laser modulated at 20 kHz, when the optical attenuation was  $1.38 \text{ m}^{-1}$ . The theoretical curve results from a numerical integration of Eq. (1). The value of  $\theta_{1/2}$  is  $1.5^\circ$ , which is about 1.7 times that expected in the farfield. These results are accurately predicted by the theoretical curve of Fig. 7. The asymmetric shape and peculiar sidelobe structure of the theoretical pattern is due to the fact that the array was

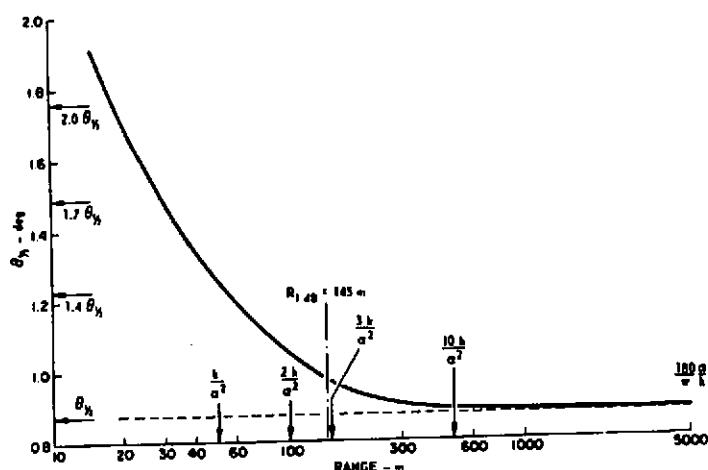


FIGURE 7  
NEARFIELD RANGE CRITERION

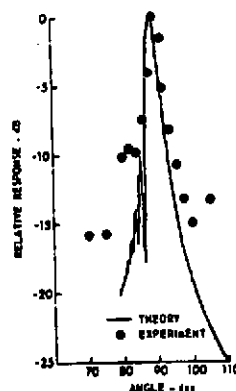


FIGURE 8  
NEARFIELD BEAMPATTERN

rotated about one end. Discrepancies between the theoretical and experimental results are probably due to the effects of reflections off the optical standpipe. However, the experimental pattern agrees quite well with theory in the vicinity of the major lobe.

#### Summary

The measurements described in this paper support the general validity of the Westervelt-Larson theory for the laser-excited thermoacoustic array. It has been shown that an acoustic signal is produced by thermalization of modulated laser light in natural fresh water, and that the sound is generated in a beam with a measured shape and beamwidth that is in reasonable agreement with theory. It has also been demonstrated that the source level is a linear function of laser power, as predicted by theory, and theoretical predictions of absolute sound pressure level have been verified experimentally. The effects of laser beam diameter on acoustic source level were examined to develop a means of determining optimum aperture radius in array design. Nearfield effects have also been formulated and confirmed experimentally.

#### Discussion

The attractiveness of the thermoacoustic array as an underwater sound source lies in its ability to produce extremely narrow beams with a minimum of underwater hardware. This is especially true for blue-green lasers, as there is an optical "window" for the transmission of light in sea water in this region of the spectrum. For example, theory predicts that a blue-green system operating in a "bi-polar" configuration (one that illuminates the medium in both the + and - z directions) would produce half-power

beamwidths ranging from a few millidegrees at 1 megahertz to a few degrees at 1 kilohertz. The effective array length for directivity considerations is roughly 36 m, which is not a small array! However, it could be developed with a relatively small optical standpipe protruding into the medium.

The main disadvantage of the thermoacoustic array is its low efficiency. To produce a source level on the order of 100 dB re 1  $\mu$ bar at 1 m, Eq. (4) can be used to show that megawatts of optical power would be required in the megahertz frequency region, with watts required in the kilohertz region. These requirements on laser power may seem extravagant at present, but this situation is likely to change with time. Blue-green laser technology is rapidly expanding,<sup>13,14</sup> and spin-offs from the nuclear fusion work should also greatly advance high power laser technology.

#### ACKNOWLEDGMENTS

This work was supported by the U.S. Navy Office of Naval Research. The authors are indebted to T. Kujawa, J. L. Guyer, and L. A. Thompson for their assistance in developing the experimental apparatus. Many helpful discussions with P. J. Westervelt are also acknowledged.

#### REFERENCES

1. P. J. Westervelt and R. S. Larson, J. Acoust. Soc. Am. 54, 121-122 (1973).
2. J. R. Clynch, L. A. Thompson, and T. G. Muir, J. Acoust. Soc. Am. 56, 824-826 (1974).
3. E. F. Carome, N. A. Clark, and C. E. Moeller, Appl. Phys. Lett. 4, No. 6, 95-97 (1964).
4. L. S. Gournay, J. Acoust. Soc. Am. 40, 1322-1330 (1966).
5. A. A. Offenberger, Phys. Lett. 34A, 62 (1971).
6. Y. Kohanzadeh, J. R. Whinnery, and M. M. Carroll, J. Acoust. Soc. Am. 57, 67-71 (1975).
7. D. C. Auth, Appl. Phys. Lett. 16 (12), 521 (1970).
8. H. Eichler and H. Stahl, IEEE J. Quan. Elec. QE8 (6), 522 (1972).
9. In the notation of Ref. 1,  $I_0$  is interpreted as the magnitude of the oscillating component of the light intensity. In the present study, the convention defining  $I_0$  as the intensity of the unmodulated laser beam has been adopted, and this convention necessitates incorporation of an additional factor of 1/2 in Eq. (1) and in subsequent formulas describing the acoustic pressure.
10. D. J. Baird and C. M. McKinney, J. Acoust. Soc. Am. 34, 1576-1581 (1962).
11. C. R. Culbertson, "Experimental Investigation of the Laser-Excited Thermoacoustic Array in Water," Masters thesis presented to the Department of Electrical Engineering, The University of Texas at Austin, Austin, Texas (May 1975).
12. R. S. Larson, "Optoacoustic Interaction in Fluids," Doctoral dissertation presented to Brown University (May 1974), p. 16.
13. C. B. Collins, A. J. Cunningham, and M. Stockton, Appl. Phys. Lett. 25 (6), 344-345 (15 September 1974).
14. G. N. Alfervov, V. I. Donin, and B. Ya. Yurshin, Zh. Eksp. Theor. Fiz. Pis'ma Red. 18 (10), 629-631 (1973).